



The following Communications have been judged by at least two referees to be “very important papers” and will be published online at www.angewandte.org soon:

X. Lang, H. Ji, C. Chen, W. Ma,* J. Zhao*

Selective Formation of Imines by Aerobic Photocatalytic Oxidation of Amines on TiO₂

K. Nakano, S. Hashimoto, M. Nakamura, T. Kamada, K. Nozaki*
Synthesis of Stereogradient Poly(propylene carbonate) by Stereo- and Enantioselective Copolymerization of Propylene Oxide with Carbon Dioxide

K. Ohmori, T. Shono, Y. Hatakoshi, T. Yano, K. Suzuki*

An Integrated Synthetic Strategy for Higher Catechin Oligomers

L. Aboshyan-Sorgho, C. Besnard, P. Pattison, K. R. Kittilstved, A. Aebischer, J.-C. Bünzli, A. Hauser,* C. Piguet*

Molecular Near-Infrared to Visible Light Upconversion in a Trinuclear d-f-d Complex

A. Donazzi, D. Livio, M. Maestri, E. Tronconi, A. Beretta,* G. Groppi, P. Forzatti

Synergy of Homogenous and Heterogeneous Processes Probed by In Situ Spatially Resolved Measurements of Temperature and Composition

C. A. Naini, S. Franzka, S. Frost, M. Ulbricht, N. Hartmann*

Probing the Intrinsic Switching Kinetics of Ultrathin Thermoresponsive Polymer Brushes

R. Linser, M. Dasari, M. Hiller, V. Higman, U. Fink, J.-M. d. Amo, S. Markovic, L. Handel, B. Kessler, P. Schmieder, D. Oesterheld, H. Oshkinat, B. Reif*

Proton-Detected Solid-State NMR Spectroscopy of Fibrillar and Membrane Proteins

X. Wurzenberger, H. Piotrowski, P. Klüfers*

A Stable Square-Planar High-Spin-d⁶ Molecular Fe^{II}O₄ Chromophore From Rare Iron(II) Minerals

Y.-G. Zhou, N. V. Rees, R. G. Compton*

Electrochemical Detection and Characterization of Silver Nanoparticles in Aqueous Solution

I. Piel, M. Steinmetz, K. Hirano, R. Fröhlich, S. Grimme,* F. Glorius*

Highly Asymmetric NHC-Catalyzed Hydroacylation of Unactivated Alkenes and Mechanistic Insights

Author Profile



“My favorite subject at school was chemistry, though I was not particularly good at it at the time!
 My greatest achievement has been mentoring a large number of very successful young scientists ...”
 This and more about Anthony K. Cheetham can be found on page 3598.

Anthony K. Cheetham — 3596–3598



S. W. Hell



K. Meerholz



B. M. Weckhuysen

News

Hansen Family Award:

S. W. Hell — 3599

Innovation Prize:

K. Meerholz — 3599

Paul H. Emmett Award:

B. M. Weckhuysen — 3599

Books

Modern Drug Synthesis

Jie Jack Li, Douglas S. Johnson

reviewed by P. Dauban — 3600

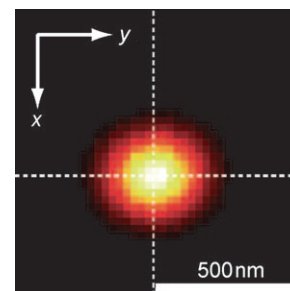
Highlights

Single-Molecule Absorption

T. Basché* ————— 3602 – 3604

Photothermal Contrast Reaches Single-Molecule Sensitivity

The detection of single-molecule absorption under ambient conditions is a very challenging task, because the tiny change in transmission is difficult to discriminate against the noise from the light beam and from scattering. By pushing the detection limits of photothermal contrast imaging, single-molecule absorption has been measured by the refraction index change induced in the environment by the heat released from the molecule (see image).

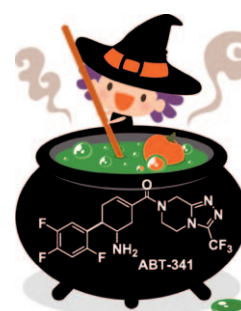


One-Pot Reactions

C. Vaxelaire, P. Winter,
M. Christmann* ————— 3605 – 3607

One-Pot Reactions Accelerate the Synthesis of Active Pharmaceutical Ingredients

All in one: A one-pot synthesis of the dipeptidylpeptidase IV selective inhibitor ABT-341 (see structure) by using an “uninterrupted sequence of reactions” has been developed. This strategy broadens the spectrum of one-pot reactions and is poised to speed up the synthesis of medicinally relevant drug compounds.

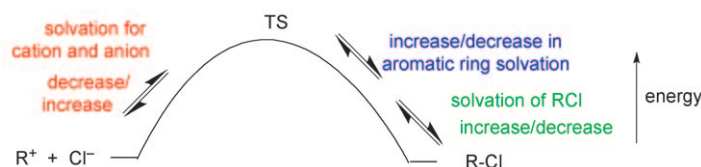


Correspondence

Structure–Reactivity Relationships

T. W. Bentley* ————— 3608 – 3611

Limitations of the $s(E+N)$ and Related Equations: Solvent Dependence of Electrophilicity



Solvent matters: Cations are reference substrates in the equation $\log k = s(E+N)$; neglect of solvent effects (see picture; TS = transition state) on their electrophilicity (E) leads to unreliable values of the nucleophilicity (N) and slope (s) parameters that characterize nucleophiles (k is the rate constant). Consequently, these parameters are not recommended for a general scale of nucleophilicity as suggested by Mayr and co-workers.

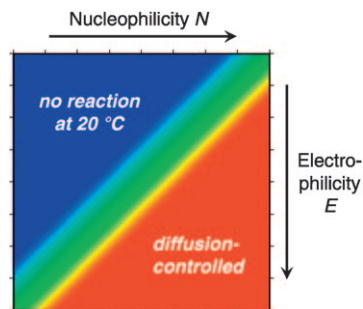
ters that characterize nucleophiles (k is the rate constant). Consequently, these parameters are not recommended for a general scale of nucleophilicity as suggested by Mayr and co-workers.

For the USA and Canada:
ANGEWANDTE CHEMIE International Edition (ISSN 1433-7851) is published weekly by Wiley-VCH, PO Box 191161, 69451 Weinheim, Germany. Air freight and mailing in the USA by Publications Expediting Inc., 200 Meacham Ave., Elmont, NY 11003. Periodicals

postage paid at Jamaica, NY 11431. US POSTMASTER: send address changes to *Angewandte Chemie*, Journal Customer Services, John Wiley & Sons Inc., 350 Main St., Malden, MA 02148-5020. Annual subscription price for institutions: US\$ 9442/8583 (valid for print and electronic / print or electronic delivery); for

individuals who are personal members of a national chemical society prices are available on request. Postage and handling charges included. All prices are subject to local VAT/sales tax.

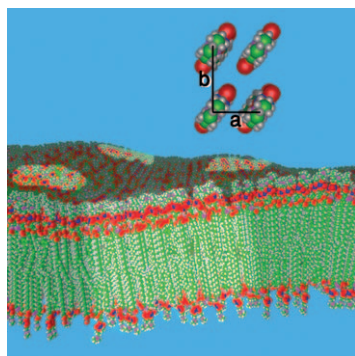
Simple and unambiguous: In the equation $\log k = s(E+N)$, the nucleophilicity N is obtained through the intercepts on the abscissa of linear $\log k$ versus E (electrophilicity) correlations. This approach places nucleophiles that differ by more than 30 orders of magnitude in reactivity on a single scale that can be used as a guide for designing organic syntheses. The equation in question is not only more practical but is also more precise than Bentley's alternatives.



Structure–Reactivity Relationships

H. Mayr* _____ 3612–3618

Reply to T. W. Bentley: Limitations of the $s(E+N)$ and Related Equations



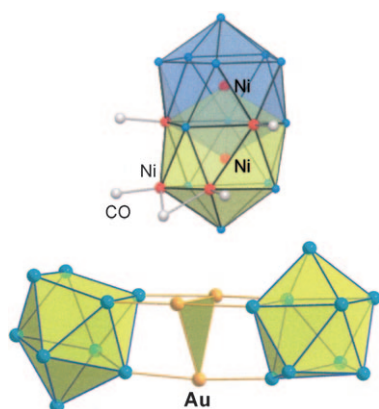
Are we all on the same raft? Membrane lipids segregate into domains. During the past two decades the structural organization of such lipid domains has been studied by several X-ray diffraction techniques. The correlation between crystalline lipid domains and lipid phases, and their relevance to functional domains in biological membranes are discussed in this Minireview.

Minireviews

Lipid Domains

R. Ziblat, L. Leiserowitz,
 L. Addadi* _____ 3620–3629

Crystalline Lipid Domains:
 Characterization by X-Ray Diffraction and
 their Relation to Biology



Zintl ions go intermetalloid: Zintl phases are mainly at home in solid-state chemistry, but their soluble representatives open fascinating possibilities as precursors for intermetalloid clusters and cage compounds. The recent upsurge of research activity in this field has now provided a rich plethora of new compounds, for example Zintl ions functionalized with organic groups, by oxidative coupling reactions, or by encapsulation of metal ions with the formation of endohedral clusters and intermetalloid compounds.

Reviews

Zintl Ions

S. Scharfe, F. Kraus, S. Stegmaier,
 A. Schier, T. F. Fässler* _____ 3630–3670

Zintl Ions, Cage Compounds, and
 Intermetalloid Clusters of Group 14 and
 Group 15 Elements

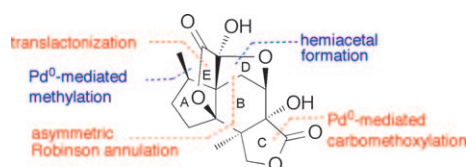
Communications

Natural Products

J. Xu, L. Trzoss, W. K. Chang,
E. A. Theodorakis* — 3672–3676



Enantioselective Total Synthesis of
(–)-jiadifenolide



1: (–)-jiadifenolide

Neurofunk: Highlights of the synthesis of **1**, a potent modulator of neurotrophic factors, include construction of the B ring through an asymmetric Robinson annulation, assembly of the E ring lactone

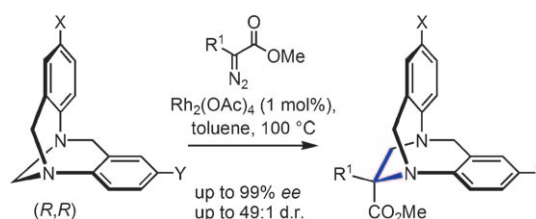
through a novel acid-induced cascade reaction, and Pd⁰-mediated carbomethoxylation and methylation reactions for the construction of the C and A rings, respectively.

Synthetic Methods

A. Sharma, L. Guénée, J.-V. Naubron,
J. Lacour* — 3677–3680



One-Step Catalytic Asymmetric Synthesis of Configurationally Stable Tröger Bases



Bridging the gap: Configurationally stable ethano-bridged Tröger bases have been prepared in a single step by the direct rhodium(II)-catalyzed reaction of methano-bridged Tröger bases and diazo esters

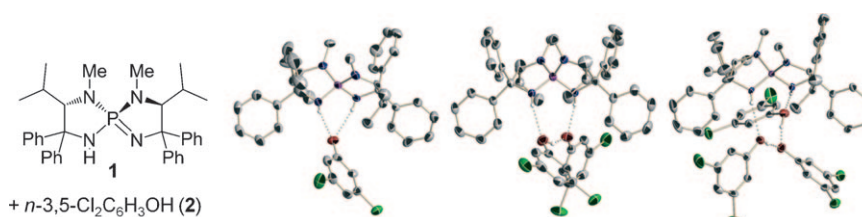
(see scheme). The process is general, enantiospecific, diastereoselective (with introduction of a new quaternary carbon center), and regioselective.

Supramolecular Catalysis

D. Uraguchi, Y. Ueki,
T. Ooi* — 3681–3683



Controlled Assembly of Chiral Tetraaminophosphonium Aryloxide–Arylhydroxide(s) in Solution



As you like it: Low-temperature ³¹P NMR spectroscopic and X-ray crystallographic analyses have revealed that chiral *P*-spiro triaminoiminophosphorane **1** and 3,5-

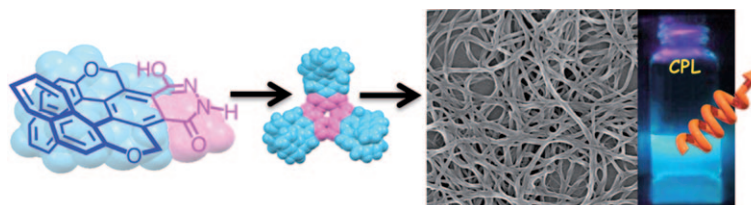
dichlorophenol (**2**) selectively assemble into three types of discrete molecular structures, **1**·**2**_{*n*} (*n* = 1–3; see picture) depending on the stoichiometry of **2**.

Self-Assembly

T. Kaseyama, S. Furumi, X. Zhang,
K. Tanaka, M. Takeuchi* — 3684–3687

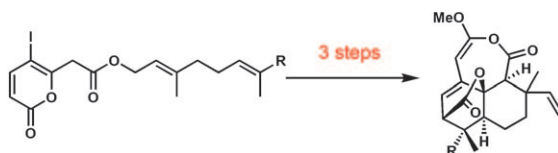


Hierarchical Assembly of a Phthalhydrazide-Functionalized Helicene



High in fiber: 1D fibrous superstructures are formed by an enantiopure phthalhydrazide-functionalized helicene in nonpolar solvents. Trimeric disks are formed by hydrogen-bonding interactions of phthal-

hydrazide units that are longitudinally interlocked for optimal packing (see picture). The resulting supramolecular assemblies exhibited large circularly polarized luminescence in solution.



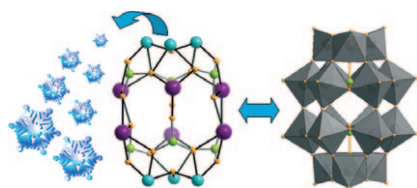
In a flash: The total synthesis of transtaganolide and basiliolide natural products is achieved in three steps from achiral, monocyclic esters (see scheme).

Featured in the syntheses are an Ireland–Claisen/Diels–Alder cascade and a novel methoxyacetylide coupling/cyclization sequence.

Natural Product Synthesis

H. M. Nelson, K. Murakami, S. C. Virgil,
B. M. Stoltz* _____ 3688–3691

A General Approach to the Basiliolide/
Transtaganolide Natural Products: Total
Syntheses of Basiliolide B, *epi*-8-
Basiliolide B, Transtaganolide C, and
Transtaganolide D



Cool stuff: The usage of phosphonates has led to formation of a family of 3d–4f heterometallic cages with a Wells–Dawson-like structure (see picture; Gd, Dy, or Y purple; Ni cyan; P green; O orange; C gray). Magnetic studies show ferromagnetic interactions within the oxo-centered nickel triangle and huge entropy change in the Gd analogue, which, in principle, can be used as an ultralow-temperature coolant.

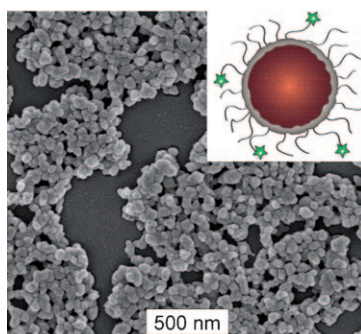
Molecular Coolers

Y.-Z. Zheng, M. Evangelisti,
R. E. P. Winpenny* _____ 3692–3695

Large Magnetocaloric Effect in a
Wells–Dawson Type $\{Ni_6Gd_6P_6\}$ Cage



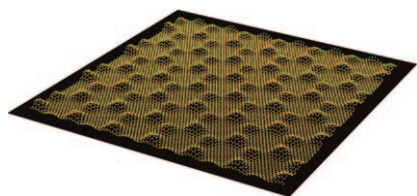
Seeing is believing: Phosphorescent nanoscale coordination polymers (NCPs) with unprecedentedly high dye loadings were coated with thin silica shells to tune the dye release kinetics (see picture). Further functionalization of the NCP/silica particles with poly(ethylene glycol) (PEG) and PEG-anisamide enhanced their biocompatibility and targeting ability, allowing cancer-specific imaging of human lung cancer H460 cells.



Functional Coordination Polymers

D. Liu, R. C. Huxford,
W. Lin* _____ 3696–3700

Phosphorescent Nanoscale Coordination
Polymers as Contrast Agents for Optical
Imaging



Directing films: The chemical vapor deposition of $(MeO)_3B$ on a multilayered Rh(111) substrate results in selective precursor decomposition leading to a boride-type film. This film can be oxidized into a well-ordered boron nitride monolayer (see picture with model structure), thus opening up a new approach to BN systems.

Boron Nitride Monolayers

H. Sachdev,* F. Müller,
S. Hüfner _____ 3701–3705

Formation of Boron-Based Films and
Boron Nitride Layers by CVD of a Boron
Ester

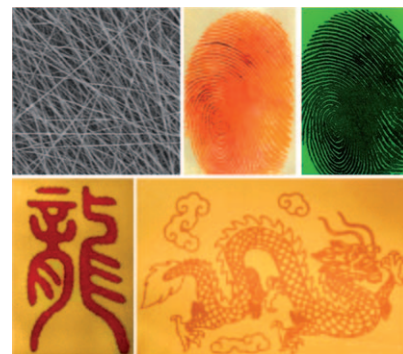
Fingerprint Recognition

S. Y. Yang, C. F. Wang,
S. Chen* _____ 3706–3709



A Release-Induced Response for the Rapid Recognition of Latent Fingerprints and Formation of Inkjet-Printed Patterns

Enter the dragon: An electrospun nanofiber mat is used to identify latent fingerprints on various surfaces within 30 seconds and produce inkjet-printed patterns. In contrast to classical approaches, the method is easy-to-operate, environmentally friendly, and has implications in other applied systems including chemical sensors, drug delivery, biological detection, and microreactors.

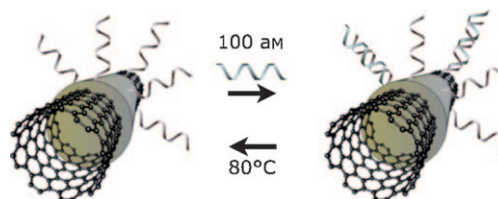


Attomolar DNA Detection

T. Kurkina, A. Vlandas, A. Ahmad, K. Kern,
K. Balasubramanian* _____ 3710–3714



Label-Free Detection of Few Copies of DNA with Carbon Nanotube Impedance Biosensors



Finding that needle in the haystack: A label-free on-chip detection strategy based on carbon nanotubes (see picture) was used to detect an oligonucleotide target sequence of which less than 2000 copies were present in a 30 μ L sample droplet,

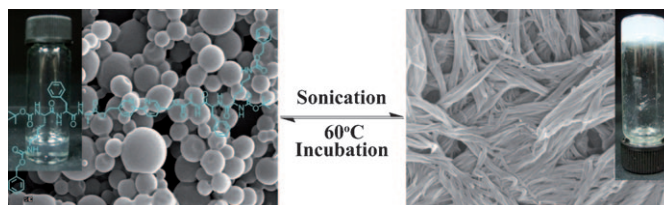
without the need for PCR. Instead, sensitive low-noise impedance measurement coupled to field-effect detection enabled attomolar DNA detection in a heterogeneous environment.

Peptide Self-Assembly

D. M. Ke, C. L. Zhan,* A. D. Q. Li,
J. N. Yao* _____ 3715–3719



Morphological Transformation between Nanofibers and Vesicles in a Controllable Bipyridine–Tripeptide Self-Assembly



Tuning structures: Stimulus-responsive peptide self-assembly requires a balance of conformational change and structural continuity of stable β sheets. In an amphiphilic bipyridine–tripeptide model, temperature, and ultrasound switch a

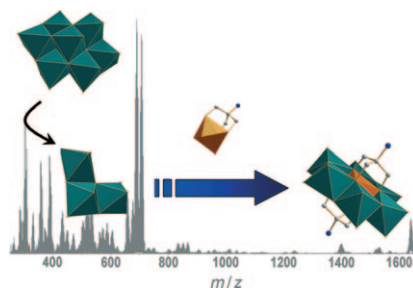
reversible morphological transformation between vesicles and nanofibers (see picture) through the synergistic effects of terminal β -sheet-forming peptides, flexible linkers, and rotatable bipyridine groups.

Organic–Inorganic Hybrid Materials

E. F. Wilson, H. N. Miras, M. H. Rosnes,
L. Cronin* _____ 3720–3724

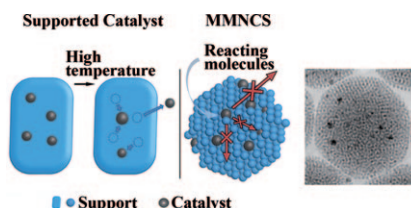


Real-Time Observation of the Self-Assembly of Hybrid Polyoxometalates Using Mass Spectrometry



Catching a glimpse: Electrospray ionization mass spectrometry (ESI-MS) allows monitoring of the real-time, “in-solution” formation of an organic–inorganic polyoxometalate hybrid system (see picture). This has provided insight into the rearrangement involved in the formation of the manganese–Anderson cluster coordinated with tris(hydroxymethyl)aminomethane ligands, through the rearrangement of the $[\alpha\text{-Mo}_8\text{O}_{26}]^{4-}$ cluster in the presence of $\text{Mn}(\text{CH}_3\text{CO}_2)_3$.

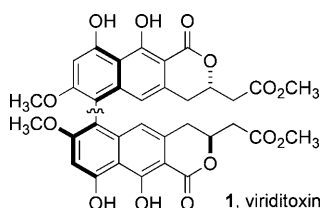
A caged catalyst: Noble-metal and oxide nanoparticles can be assembled to obtain high-temperature-stable mesoporous multicomponent nanocomposite colloidal spheres (MMNCSs; see picture). CO oxidation and cyclohexene hydroconversion were selected to examine the catalytic activity, selectivity, and thermal stability of these MMNCSs. The exhibited catalytic properties suggest that the reported MMNCSs are ideal model catalysts for high-temperature reactions.



Heterogeneous Catalysis

C. Chen, C. Nan, D. Wang, Q. Su, H. Duan, X. Liu, L. Zhang, D. Chu, W. Song, Q. Peng, Y. Li* — **3725–3729**

Mesoporous Multicomponent Nanocomposite Colloidal Spheres: Ideal High-Temperature Stable Model Catalysts

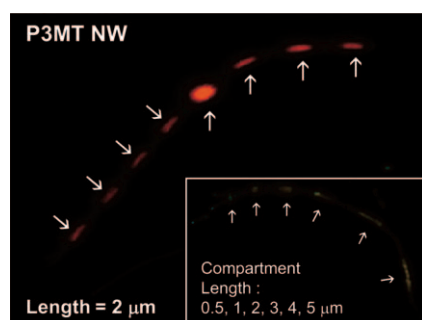


Remote control: Vanadium catalysts provide the key to synthesizing the bacteria-fighting natural product viriditoxin. An achiral catalyst shows modest levels of remote diastereocontrol induced by the lactone stereogenic center and chiral catalysts can be used to enhance or reverse this inherent selectivity.

Natural Product Synthesis

Y. S. Park, C. I. Grove, M. González-López, S. Urgaonkar, J. C. Fetting, J. T. Shaw* — **3730–3733**

Synthesis of (–)-Viriditoxin: A 6,6'-Binaphthopyran-2-one that Targets the Bacterial Cell Division Protein FtsZ

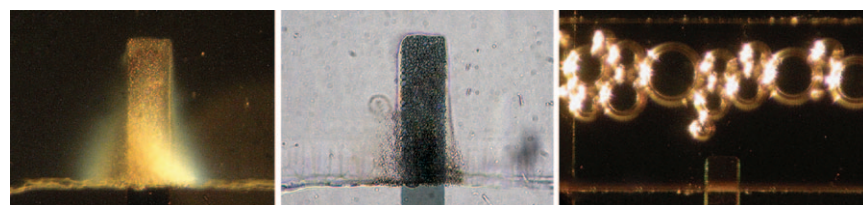


Let your little light shine: Light-emitting organic poly(3-methylthiophene) (P3MT) and inorganic titanium dioxide single nanowires (NWs) treated with focused electron beams have multiple 1D serial compartments (see picture) similar to superlattice NWs, which are applicable to light-emitting color barcode NWs. The structural, optical, and electrical properties of the treated NW compartments can be controlled through the irradiation conditions.

Nanoscale Tailoring

Y. K. Hong, D. H. Park, S. G. Jo, M. H. Koo, D.-C. Kim, J. Kim, J. S. Kim, S. Y. Jang, J. Joo* — **3734–3738**

Fine Characteristics Tailoring of Organic and Inorganic Nanowires Using Focused Electron-Beam Irradiation



Visible to the naked eye: An interplay between microscale electrophoresis and electrochemistry was exploited to simultaneously confine macromolecular encapsulants near an electrode surface while inflating them with gases evolved from the electrochemical reactions local-

ized there. The compacted film can be seen under ordinary white light even when samples are unlabeled thus enabling a label-free technique for the detection of a variety of macromolecules including DNA, proteins, and cyclodextrans.

Microbubbles

Y.-W. Huang, F. A. Shaikh, V. M. Ugaz* — **3739–3743**

Tunable Synthesis of Encapsulated Microbubbles by Coupled Electrophoretic Stabilization and Electrochemical Inflation

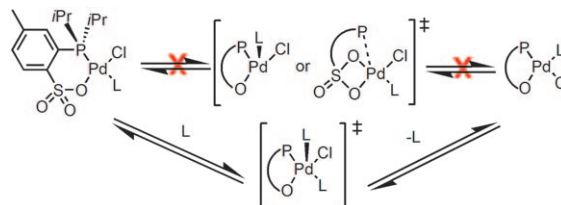


Homogeneous Catalysis

M. P. Conley, R. F. Jordan* – 3744–3746



cis/trans Isomerization of Phosphinesulfonate Palladium(II) Complexes



With a little help from a friend: Chain growth in olefin polymerization by $[\{PO\}PdR]$ catalysts is believed to occur by unimolecular *cis*-*P,R*- to *trans*-*P,R*- $[\{PO\}PdR(olefin)]$ isomerization, with subsequent insertion. Studies with

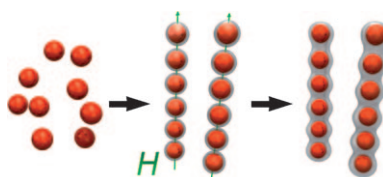
$[\{PO\}Pd(py)_2]^+$ (py = pyridine) and non-equilibrium *cis/trans* mixtures of $[\{PO\}PdClP(O-o-tolyl)_3]$ indicate that an external ligand is necessary for *cis/trans* isomerization of $\{PO\}Pd$ complexes (see scheme). $\{PO\}$ = 2-Phosphinosulfonate.

Magnetic Nanomaterials

Y. Hu, L. He, Y. Yin* – 3747–3750



Magnetically Responsive Photonic Nanochains



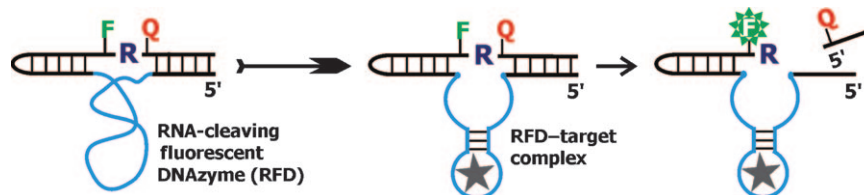
Nano-peapods: Magnetically responsive photonic nanochains have been produced by inducing chain alignment of uniform magnetic particles during their silica coating process and then allowing additional deposited silica to wrap entire structures. The optical diffraction of these nanochains can be switched on and off by applying magnetic fields.

Biosensors

M. M. Ali, S. D. Aguirre, H. Lazim, Y. Li* – 3751–3754



Fluorogenic DNAzyme Probes as Bacterial Indicators



Lighting up bacteria: An RNA-cleaving fluorescent DNAzyme (RFD) can produce a fluorescent signal in the crude extracellular mixture generated by live bacterial cells (see picture). These DNAzymes

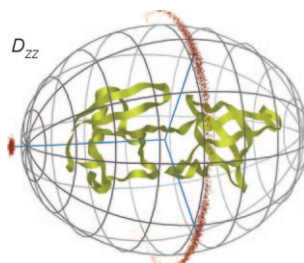
cleave a lone RNA linkage (R) embedded in a DNA chain and flanked by nucleotides labeled with a fluorophore (F) and a quencher (Q).

NMR Spectroscopy

L. Salmon, J.-L. Ortega Roldan, E. Lescop, A. Licinio, N. van Nuland, M. R. Jensen,* M. Blackledge* – 3755–3759

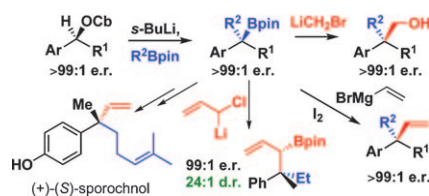


Structure, Dynamics, and Kinetics of Weak Protein–Protein Complexes from NMR Spin Relaxation Measurements of Titrated Solutions



Making the invisible visible: Weak protein–protein interactions play a key role in a range of essential biological processes. However, transient or ultraweak complexes cannot be studied in detail by many biophysical techniques. A method based on the measurement of ^{15}N relaxation rates can be used to study weak protein complexes (see picture; D_{zz} = diffusion tensor).

Pin it down: A range of substrates that bear versatile functional groups with quaternary stereogenic centers have been prepared with very high enantioselectivity from tertiary boronic esters (see scheme; Cb = *N,N*-diisopropylcarbamoyl, pin = pinacolato). The preparation of allylboronic esters bearing contiguous quaternary and tertiary stereogenic centers, and applications to natural product synthesis are also reported.

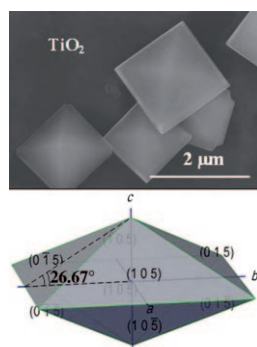


Quaternary Centers

R. P. Sonawane, V. Jheengut, C. Rabalakos, R. Larouche-Gauthier, H. K. Scott, V. K. Aggarwal* . 3760–3763

Enantioselective Construction of Quaternary Stereogenic Centers from Tertiary Boronic Esters: Methodology and Applications

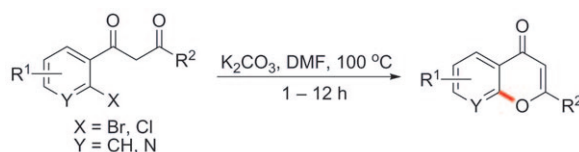
Put your best face forward: The performance of TiO₂ anatase crystals in energy and environmental applications is normally correlated with the TiO₂ crystal facets exposed, and increasing the percentage of highly reactive surfaces is extremely important. A new gas-phase oxidation process using TiCl₄ as precursor now yields anatase TiO₂ single crystals with primarily high-index {105} facets, which can cleave water photocatalytically.



High-Index Facets

H. B. Jiang, Q. Cuan, C. Z. Wen, J. Xing, D. Wu, X. Q. Gong, C. Li,* H. G. Yang* . 3764–3768

Anatase TiO₂ Crystals with Exposed High-Index Facets



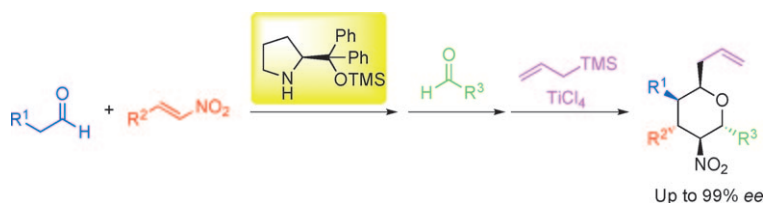
Expect the unexpected: A transition-metal-free approach to access chromone derivatives has been developed. The intramolecular O-arylation of substituted 1-(2-haloaryl)-propane-1,3-diones in DMF

in the presence of K₂CO₃ gave the corresponding target products in good to excellent yields (see scheme; DMF = *N,N'*-dimethylformamide).

Oxygen Heterocycles

J. Zhao, Y. Zhao, H. Fu* . 3769–3773

Transition-Metal-Free Intramolecular Ullmann-Type O-Arylation: Synthesis of Chromone Derivatives



Domino effect: The title reaction uses an asymmetric Michael/Henry reaction/acylation/Lewis acid mediated allylation reaction to provide highly substituted tetrahydropyrans with excellent enantioselectivity (see scheme; TMS = tri-

methylsilyl). All the carbon atoms in the tetrahydropyran ring are substituted with different groups, and the relative and absolute stereochemistry of the five contiguous carbon centers are completely controlled.

Organocatalysis

H. Ishikawa, S. Sawano, Y. Yasui, Y. Shibata, Y. Hayashi* . 3774–3779

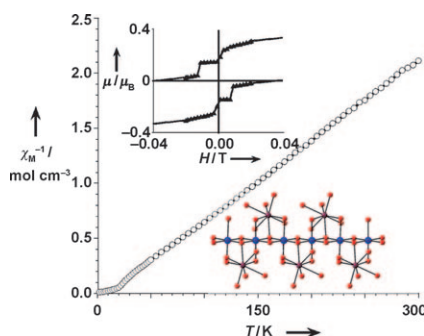
Asymmetric One-Pot Four-Component Coupling Reaction: Synthesis of Substituted Tetrahydropyrans Catalyzed by Diphenylprolinol Silyl Ether

Ferromagnetic Materials

J. P. West, W. L. Queen, S.-J. Hwu,*
K. E. Michaux ————— **3780–3783**



Spaced Heterometallic 3d–4f Magnetic Chains from the Pseudo-One-Dimensional $\text{Na}_2\text{LnMnO}(\text{AsO}_4)_2$ Series: Stepped Magnetization in the $\text{Na}_2\text{GdMnO}(\text{AsO}_4)_2$ Ferromagnet



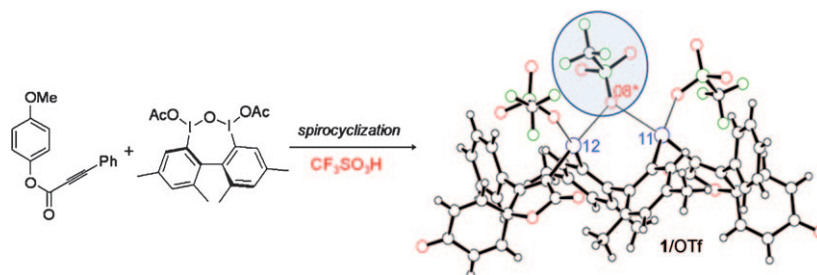
Step it up: The $\text{Na}_2\text{LnMnO}(\text{AsO}_4)_2$ series contains Ln-capped $[\text{MnO}_4]_\infty$ ferromagnetic chains, and the species with Ln = Gd reveals intriguing magnetic anomalies thought to be attributed to better structural confinement of the magnetic chains. It exhibits stepped magnetization and multiple-spin dynamics (see picture; Mn blue, Gd maroon, O red), two phenomena never before observed in a quasi-one-dimensional, 3d–4f condensed solid.

Hypervalent Compounds

T. Dohi, D. Kato, R. Hyodo, D. Yamashita,
M. Shiro, Y. Kita* ————— **3784–3787**



Discovery of Stabilized Bisiodonium Salts as Intermediates in the Carbon–Carbon Bond Formation of Alkynes



Ways and means to spirocycles: Pseudocyclic bisiodonium salts **1** stabilized by a secondary bonding interaction—an $\text{I}^{\text{III}}\cdots\text{O}\cdots\text{I}^{\text{III}}$ pseudobridge linkage (circle)—were prepared by C–C bond formation between aryl alkynes and a μ -oxo-bridged

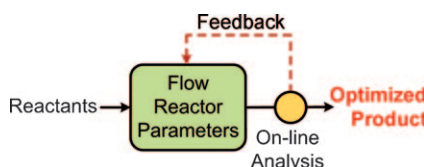
hypervalent iodine compound. The synthetic utility of salts **1** was demonstrated by their facile conversion into functionalized spirocycles by treatment with a nucleophile.

Reaction Optimization

A. J. Parrott, R. A. Bourne, G. R. Akien,
D. J. Irvine,* M. Poliakoff* — **3788–3792**



Self-Optimizing Continuous Reactions in Supercritical Carbon Dioxide



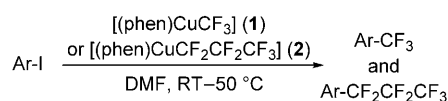
Hands-free optimization: A combination of an automated flow reactor, online analysis, and a control algorithm leads to efficient optimization of reactions to a given product without the need for human intervention.

Trifluoromethylation

H. Morimoto, T. Tsubogo, N. D. Litvinas,
J. F. Hartwig* ————— **3793–3798**



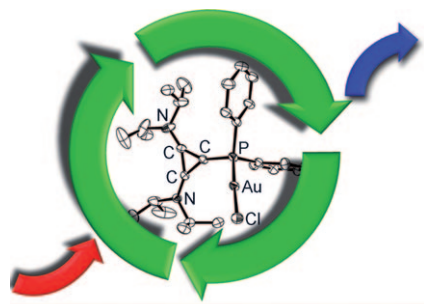
A Broadly Applicable Copper Reagent for Trifluoromethylations and Perfluoroalkylations of Aryl Iodides and Bromides



- Scope encompasses electron-neutral, -rich, and -deficient ArI
- Compatible with COCH_3 , CHO , CO_2Me , CH_2OH , NO_2 , NHC(O)OMe , CN , Br

Well compatible: The trifluoromethylations and perfluoroalkylations of aryl iodides and some aryl bromides with trifluoromethyl and perfluoroalkylcopper(I) phenanthroline complexes occur with broad scope at 25–50 °C (see

scheme). The trifluoromethyl complex is prepared from inexpensive reagents and can be used in situ or isolated. The reactions tolerate a range of substituents and also occur with heteroaromatic systems.

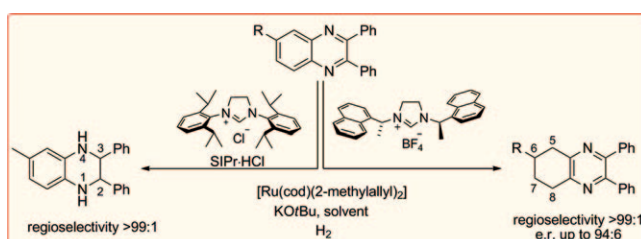


Cationic but electron-rich: Cyclopropenyliidene-stabilized phosphonium cations exhibit the electron richness of classical trialkyl and triaryl phosphines even though they carry a positive charge stemming from a cationic substituent directly bonded to the phosphorous atom. These two facts have been exploited to synthesize gold catalysts that can be easily recycled after use.

Ligand Design

J. Petušková, H. Bruns,
 M. Alcarazo* _____ 3799 – 3802

Cyclopropenyliidene-Stabilized Diaryl and Dialkyl Phosphonium Cations: Applications in Homogeneous Gold Catalysis



Inflating flat bicycles: Proper choice of the N-heterocyclic carbene (NHC) ligand in Ru NHC complexes allows the completely regioselective ligand-controlled hydrogenation of either the heterocyclic or the carbocyclic ring of a substituted quinoxaline in quantitative yields. Chiral NHC

ligands allow the challenging asymmetric hydrogenation of the carbocyclic ring of quinoxalines, yielding enantioenriched 5,6,7,8-tetrahydroquinoxalines with an enantiomeric ratio of up to 94:6.

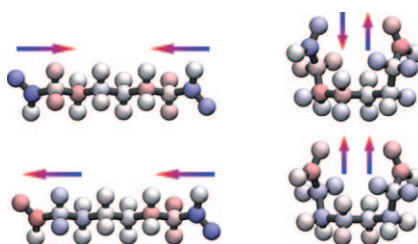
Asymmetric Hydrogenation

S. Urban, N. Ortega,
 F. Glorius* _____ 3803 – 3806

Ligand-Controlled Highly Regioselective and Asymmetric Hydrogenation of Quinoxalines Catalyzed by Ruthenium N-Heterocyclic Carbene Complexes



The relationship between conformational changes of substrate dianions in water clusters and the corresponding spectroscopic characteristics were studied theoretically and by IR spectroscopy (see picture for the charge displacement associated with the excitation of the carboxylate symmetric stretching modes). Folded structures are stabilized by the formation of additional hydrogen bonds between the solvated dianion and H₂O molecules and should thus be retained in larger, microhydrated clusters.



Solvent-Mediated Folding

T. Wende, M. Wanko, L. Jiang, G. Meijer,
 K. R. Asmis,* A. Rubio* _____ 3807 – 3810

Spectroscopic Characterization of Solvent-Mediated Folding in Dicarboxylate Dianions

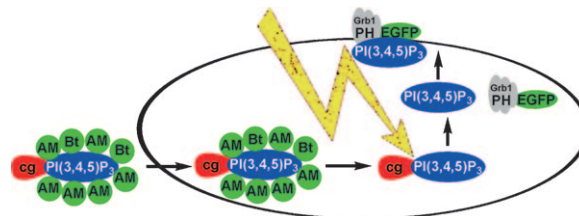


Signal Transduction

M. Mentel, V. Laketa, D. Subramanian,
H. Gillandt, C. Schultz* — 3811–3814



Photoactivatable and Cell-Membrane-Permeable Phosphatidylinositol 3,4,5-Trisphosphate



Unleashed inside cells: The signaling molecule PI(3,4,5)P₃ is prepared in a form that allows its cellular uptake and subsequent activation by light (see picture). The rapid eight-step synthetic sequence yields

a stable derivative of the signaling molecule with high biological activity after deprotection (“uncaging”) with a laser flash, in live cells.



Supporting information is available on www.angewandte.org (see article for access details).



A video clip is available as Supporting Information on www.angewandte.org (see article for access details).



This article is available online free of charge (Open Access)

Sources

Product and Company Directory

You can start the entry for your company in “Sources” in any issue of *Angewandte Chemie*.

If you would like more information, please do not hesitate to contact us.

Wiley-VCH Verlag – Advertising Department

Tel.: 0 62 01 - 60 65 65

Fax: 0 62 01 - 60 65 50

E-Mail: MSchulz@wiley-vch.de

Service

Spotlight on Angewandte's
Sister Journals — 3592–3594

Vacancies — A23

Preview — 3815

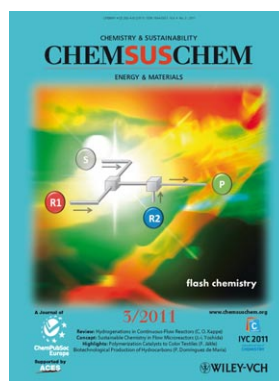
Check out these journals:



www.chemasianj.org



www.chemmedchem.org



www.chemsuschem.org



www.chemcatchchem.org